SLOW MAGNETO-ACOUSTIC WAVES IN CORONAL LOOPS

E. Verwichte[1], V.M. Nakariakov[2], D. Berghmans[1], and J.-F. Hochedez[1]

[1] *Royal Observatory of Belgium, Ringlaan 3, 1180 Brussel, Belgium*

tel: +32(0)2 3730220 / fax: +32(0)2 3730224

[2] *Physics Department, University of Warwick, Coventry, CV4 7AL, UK*

tel: +44(0)2476 522235 / fax: +44(0)2476 692016

e-mail: erwinv@oma.be, valery@astro.warwick.ac.uk, david@oma.be, hochedez@oma.be

ABSTRACT

This paper compares a high-cadence observation of propagating slow magneto-acoustic waves in large transequatorial coronal loops with a one-dimensional, analytical model. We use the TRACE and EIT sequences of the JOP80 dataset. The model describes the propagation of weakly nonlinear slow magneto-acoustic waves in a dissipative, stratified coronal loop of varying cross-section. This is the principle of coronal seismology. From the simultaneous observation of propagating waves along the same loop path, at two different temperature bandpasses, it is concluded that loops of different temperature coexist within at least 3600 km. Furthermore, the comparison between an observed wave amplitude profile with the analytical model gives a first observational estimate of the dissipation processes of parallel thermal conduction and compressive dynamical viscosity, and is shown to be in agreement with the theoretical expectations.

1. INTRODUCTION

The appearance of instruments such as SXT, EIT and TRACE enabled the detection of the spatial signatures of magnetohydrodynamic wave phenomena in coronal loop structures (*e.g.* DeForest and Gurman, 1998; Berghmans and Clette, 1999, and Aschwanden *et al.*, 1999), while before only temporal signatures could be achieved (see *e.g.* Aschwanden *et al.*, 1999 for an extended list of references). In particular, propagating slow magnetoacoustic waves have been observed in coronal structures, such as polar plumes (Ofman *et al.*, 1997 with UVCS; Deforest and Gurman, 1998 with EIT) and large coronal loops (Berghmans and Clette, 1999 with EIT; Robbrecht *et al.* (1999) with EIT and TRACE; De Moortel *et. al*, 2000 with TRACE; Berghmans, McKenzie and Clette, 2001 with SXT; Robbrecht *et al.*, 2001 with EIT and TRACE).

The corona of the sun is a highly structured medium where the emitting corona is contained in magnetic loops (*e.g.* Bray *et al* 1991). Slow magneto-acoustic waves are restricted to propagate along magnetic structures. This makes them a valuable tool for probing coronal loops. One can make the parallel with the human characteristic of wanting to put a gift-wrapped present next to one's ear and shake it to get a hint of its contents. Similarly we wish to observe the corona's response to a perturbation and by comparing with theoretical models, obtain information about its properties. This is coronal seismology. Slow magneto-acoustic waves provide information on the properties of coronal loops such as their geometry, temperature, fine-structuring and dissipation rates. This last item is of great importance to the coronal heating problem as an input to heat dissipation models.

This paper compares the observation of propagating slow magneto-acoustic waves in a large loop arcade in the temperature range of 1 MK and 1.6 MK (Robbrecht *et al.*, 2001) with a one-dimensional, analytical model of slow magneto-acoustic waves in a stratified, dissipative atmosphere. This model is similar to that of Ofman, Nakariakov and Sehgal *et al.* (2000) for coronal polar plumes and that of Nakariakov *et al.* (2001) for coronal loops.

The paper is structured as follows: In Sections 2 and 3 the analytical model and the observations are descriped respectively. In the Discussion we compare the model to the observations and deduce a value for the dissipation rate. We conclude with a discussion on the instrumental needs for optimally observing such wave phenomena in context of the future Solar Orbiter mission.

2. ANALYTICAL MODEL

Slow magneto-acoustic waves which propagate strictly along the magnetic field that traces the coronal loop (z-direction) are modelled. The loop cross-section $A(z)$ may vary arbitrarily along the loop length. We take into account dissipative contributions. The importance of inertial terms to the thermal diffusion, kinematic viscosity and magnetic difussion are given by the Péclet number, Pe, Reynolds number, Re, and magnetic Reynolds number, Rm, respectively. For typical coronal conditions and using theoretical models (Braginskii, 1965), Pe $= 10^2$, Re $= 10^4$ and Rm $= 10^{14}$. We include parallel thermal conduction and compressive viscosity. Magnetic diffusion is of interest for modelling currents sheets, which we do not consider here. The plasma motions are described by the equations

$$\frac{\partial \rho}{\partial t} + \frac{1}{A}\frac{\partial}{\partial z}(A\rho V) = 0, \tag{1}$$

$$\rho\left(\frac{\partial V}{\partial t} + V\frac{\partial V}{\partial z}\right) + \frac{\partial p}{\partial z} + g\rho = \frac{4}{3A}\frac{\partial}{\partial z}\left(A\,\eta_0\,\frac{\partial V}{\partial z}\right), \tag{2}$$

$$\frac{\partial p}{\partial t} + V\frac{\partial p}{\partial z} + \frac{\gamma p}{A}\frac{\partial}{\partial z}(AV) = \frac{(\gamma-1)}{A}\frac{\partial}{\partial z}\left(A\,\kappa_{||}\,\frac{\partial T}{\partial z}\right), \tag{3}$$

where ρ, V, p and T are the plasma density, velocity, pressure and temperature respectively. The parameter γ is the adiabatic index. The variables η_0 and $\kappa_{||}$ are the compressive, dynamic viscosity coefficient and the parallel thermal conduction coefficient respectively. They both depend on temperature as $T^{5/2}$ (Braginskii, 1965). The variable g is the component of the gravitational acceleration parallel to the magnetic field, and depends on the angle between the magnetic field direction and solar surface, and on the distance to the sun center: $g(z) = g_\odot\, dh/dz\, (1 + h/R_\odot)^{-2}$, where $h(z)$ is the height above the solar surface, $g_\odot$ is the gravitational acceleration at the solar surface and $R_\odot$ is the radius of the sun.

A static, isothermal atmosphere is chosen so that the equilibrium condition is restricted to the barometric equation

$$\frac{d\rho_0}{dz} = -\frac{\rho_0}{H(z)} \text{ or } \frac{\rho_0(z)}{\rho_0(0)} = \exp\left(-\int_0^z \frac{dz'}{H(z')}\right) \tag{4}$$

where the index '0' denotes an equilibrium quantity. The quantity $H(z) = C_s^2(\gamma g(z))^{-1}$ is the density scale-height, C_s is the thermal soundspeed, which is constant. We assume the coronal plasma to be an ideal gas.

We consider perturbations from the equilibrium: $V = V'$, $\rho = \rho_0 + \rho'$, $p = p_0 + p'$, $T = T_0 + T'$. We make the following assumptions:

1) Weakly nonlinear perturbations: $\epsilon \sim V'/C_s \ll 1$. Therefore terms in Equations (1-3) which are of order equal or higher than ϵ^3 are neglected.

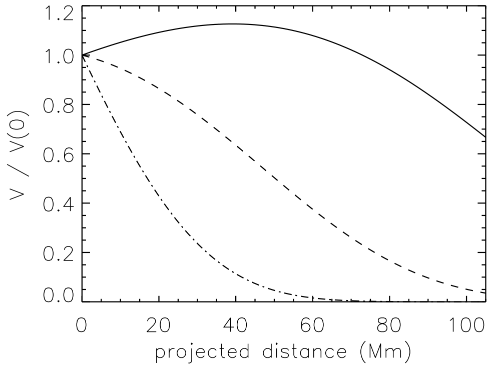

Figure 1. The relative amplitude $\hat{V}/\hat{V}(0)$ as a function of projected distance along a straight loop ($h(Z)$ = $sin(\pi/4)Z$). The loop cross-section is constant. solid line: η = 0.3 Mm, dashed line: η = 1.0 Mm, dot-dashed line: η = 3.0 Mm. $\rho_0(0)$ = 8 10^{-13} kg m^{-3}, T_0 = 1 MK and k = 2π / (C_s 300 s).

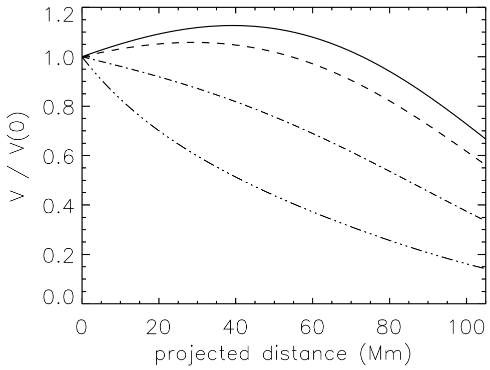

Figure 2. The relative amplitude $\hat{V}/\hat{V}(0)$ as a function of projected distance along a straight loop ($h(Z)$ = $sin(\pi/4)Z$) with the loop cross-section $A(Z)$ = $A(0)$ $(1 + (2^{n/2} - 1)Z/\Delta Z)^2$. dotted line: n=0 (constant cross-section), dotted line: n=1, dot-dashed line: n=2 and dotted-dashed line: n=3. (η = 0.3 Mm, $\rho_0(0)$ = 8 10^{-13} kg m^{-3}, T_0 = 1 MK and k = 2π / (C_s 300 s)).

2) Weakly dissipative medium: dissipative terms are considered to be of the order of ϵ^2.

3) Weak stratification: $\lambda \ll H$, the typical wavelength of the perturbation is much shorter than the density scale-height. We assume that the ratio λ/H is of the order of ϵ. We introduce new independent variables, which take into account the two different spatial scales: $\xi = z - C_s t$, $Z = \epsilon z$.

Considering these assumptions, Equations (1-3) are reduced to a modified Burgers equation for the velocity amplitude V', that governs the evolution of slow magneto-acoustic waves propagating along a coronal loop:

$$\frac{\partial V'}{\partial Z} - \frac{1}{2H}V' + \frac{1}{2A}\frac{dA}{dZ}V' + \frac{\gamma+1}{2C_s}V'\frac{\partial V'}{\partial \xi} - \frac{\eta}{2}\frac{\rho_0(0)}{\rho_0(Z)}\frac{\partial^2 V'}{\partial \xi^2} = 0 \ . \quad (5)$$

For the details of the derivation of the previous equation, we refer to Nakariakov *et al.* (2000), where the derivation procedure is the same, except that the loop cross-section was kept fixed. The second, third, fourth and fifth term of the previous equation represent, respectively, the influence of the density stratification, loop cross-section variability, nonlinearity anddissipation on the slow magneto-acoustic wave evolution. The dissipation coefficient η is defined as

$$\eta(T_0) = \frac{1}{\rho_0(0)C_s}\left(\frac{4}{3}\eta_0 + \frac{(\gamma-1)^2}{C_p}\kappa_{||}\right) . \quad (6)$$

C_p is the heat capacity at constant pressure. We can rewrite Definition (6) as $\eta/\ell \sim 4/3\,\mathrm{Re}^{-1} + (\gamma-1)^2\,\mathrm{Pe}^{-1}$, where ℓ is a typical length-scale (*e.g.* the density scale-height or solar radius). From theoretical considerations (Braginskii, 1965) and using typical coronal values ($\rho_0(0) = 8\ 10^{-13}$ kg m^{-3}, $T_0 = 10^6$ K), we estimate the value of η. For isothermal conditions (γ=1), $\eta/\ell \sim 10^{-4}$ (η = 0.08 Mm). If thermal conduction is included, the value of η may increase by two orders of magnitude. We can thus state that $\eta/\ell \gtrsim 10^{-4}$.

If we neglect the nonlinear term in Equation (5), and assume that $V'(Z,\xi) = \hat{V}(Z)\,cos(k\xi)$, we find the following solution:

$$\frac{\hat{V}(Z)}{\hat{V}(0)} = \frac{1}{\sqrt{\frac{\rho_0(Z)}{\rho_0(0)}}}\frac{1}{\sqrt{\frac{A(Z)}{A(0)}}}\mathrm{e}^{-\frac{\eta k^2}{2}\int_0^Z \frac{\rho_0(0)}{\rho_0(Z')}dZ'} , \quad (7)$$

which consists of three competing factors. Firstly, the density stratification makes the wave amplitude grow with height. Secondly, the expansion of the loop cross-section makes the wave amplitude decay with height. Lastly, the dissipation makes the wave amplitude decay with height as well. The rate of dissipation is a function of the wavenumber. Waves of shorter wavelengths (larger wavenumber) are more strongly dissipated than long wavelength waves. The condition for waves not to grow, but always to decay with height is given by:

$$k > \frac{1}{\sqrt{\eta}}\sqrt{\frac{1}{H(0)} - \left(\frac{1}{A}\frac{dA}{dZ}\right)(0)} \ . \quad (8)$$

Figure 1 shows the relative amplitude $\hat{V}/\hat{V}(0)$ as a function of the projected distance, for three values of the dissipation coefficient η. The loop is straight and the loop cross-section is constant. We consider the wavevector k corresponding to an oscillation period of 5 minutes. In function of η, Condition (8) is fulfilled if $\eta > 1$ Mm. Therefore in the case of η = 0.3 Mm the wave first grows in amplitude before decaying, while in case of η = 3 Mm, the wave always decays with height.

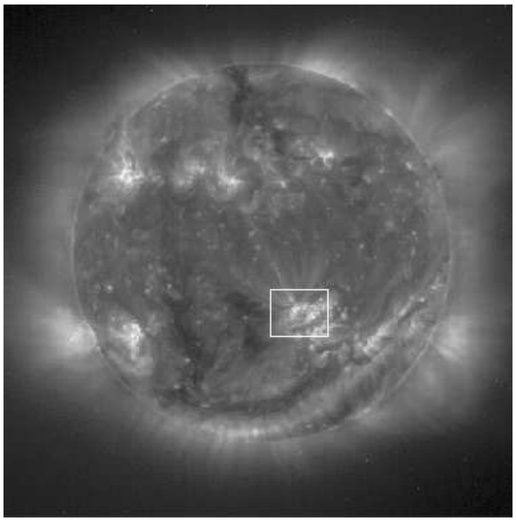

Figure 3. EIT full disk image at 195 Åbandpass, taken at 18h34m UT. The field of view of the EIT (and approximately also the TRACE) sequence around AR8218 is highlighted.

The effect of the loop cross-section is that a wave which would otherwise first grow in amplitude with height, may always decay with height if the loop expands sufficiently. This expanse can be solarge that the waves of all wavelengths decay with height. The effect of varying the loop cross-section is illustrated in Figure 2, where all parameters have the same values as before and with η = 0.3 Mm. The loop cross-section is given as $A(Z) = A(0)$ $(1 + (2^{n/2} - 1)Z/\Delta Z)^2$, where the loop cross-section increases by a factor of 2^n over the length range ΔZ. Again using Condition (8), we deduce the minimum value of n for which the wave always decays with height. This minimum value increases with η. In this specific case, we need $n \gtrsim 2$.

3. OBSERVATIONS

In the context of JOP80, the Extreme ultraviolet Imaging Telescope (EIT) on board of the SoHO, the Transition Region and Coronal Explorer (TRACE) and the Soft X-ray Telescope on board of Yohkoh, made, on May 13 1998, almost simultaneously, a high-cadence observation of the active region AR8218. This project was intended for a multi-wavelength study of bright structures (such as active region transient brightenings) with the highest possible time resolution (Berghmans and Clette, 1999; Berghmans *et al.*, 2001). This dataset lead to the first spatially resolved detection of slow magneto-acoustic waves in large coronal loops (Berghmans & Clette, 1999; Robbrecht *et al.*, 1999; Robbrecht *et al.*, 2001). For the details of the image processing of the EIT and TRACE data, The most important

Table 1. Characteristics of the EIT and TRACE sequences.

instrument	EIT	TRACE
wavelength bandpass	195 Å	171 Å
temperature bandpass	1.6 MK	1.0 MK
speed of sound	192 km s^{-1}	152 km s^{-1}
cadence	15 s	25 s
pixelsize	2.59 "	0.49 "
start time	17h31m50s	17h03m28s
end time	18h29m07s	18h07m17s
number of images	229	147

facts of these observations are given in table 1.

Robbrecht *et al.* (2001) examined propagating intensity perturbations (PDs) along large coronal loops, which emanate from the north-eastern side of the active region, and connect with active regions in the opposite hemisphere. They conclude that the PDs are slow magneto-acoustic waves. The loop length is estimated to be 800 Mm. The EIT and TRACE sequences observe only up to a quarter of the loop length (see Figures 3 and 4). The following observations of the PDs are made:

- The propagation direction along the loop is always upwards and away from the active region.
- The projected propagation speed is in the range of 65-150 km s^{-1}, which is below the speed of sound at the temperature bandpass of the observations.
- From the comparison between the projected propagation speed with the speed of sound the angle between the loop and the solar surface is deduced. Over the distance the PDs are observed, this angle is approximately constant and in the range of 30-70 degrees. This is consistent with the measured loop angle when the loop is over the solar limb some days later.
- The PDs are quasi-periodic with a period range of 5-20 minutes, which is below the acoustic cut-off period.
- The relative intensity amplitude is 8-12 % of the background intensity.
- The relative intensity decreases with distance at a scale proportional to the density scale-height. This explains why no waves are observed propagating towards the loop footpoint.

Figure 4. Field of view of the TRACE observation with the selected loop path highlighted. The image is an average over 147 individual exposures.

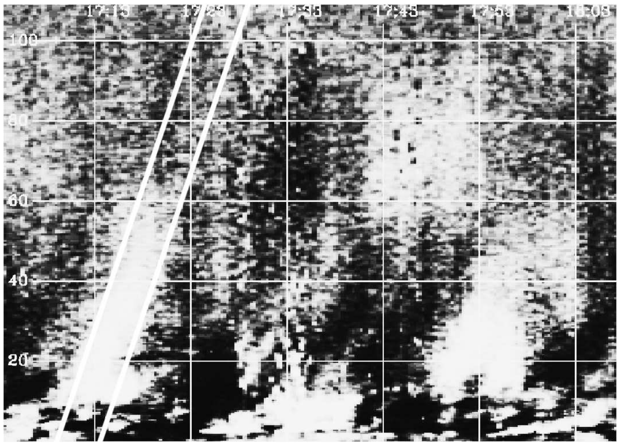

Figure 5. Loop intensity variation for the TRACE sequence, along the selected loop path as a function of time horizontally and the projected distance vertically. The time step between two vertical lines is 10 minutes and the distance step between two horizontal lines is 20 Mm.

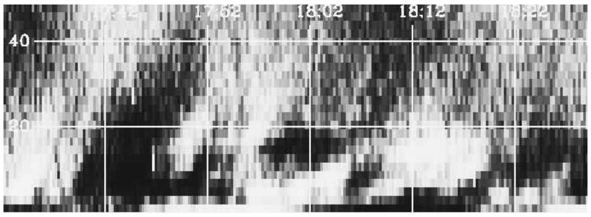

Figure 6. Loop intensity variation for the EIT sequence, along the same selected loop path as a function of time horizontally and the projected distance vertically. Note that the EIT sequence begins approximately half an hour later than the TRACE sequence.

These observations validate the use of a model with weakly nonlinear, dissipative waves, but which are only marginally weakly stratified.

Robbrecht *et al.* (2001) observed the simultaneous propagation of slow waves in TRACE (at 1 MK) and EIT (at 1.6 MK) along the same path on the solar disk. This is illustrated in Figures 5 and 6 The path in the two instruments is co-aligned to within an accuracy of 1-2 EIT pixels (1800-3600 km). The propagation speed in the EIT sequence is systematically faster than in the TRACE sequence. By assuming that the observed propagation speed is the projected speed of sound at that temperature, the angle of the coronal loop with the solar surface is found. For both instruments, we find approximately the same consistent angle. Thus, the two waves travel through the same volume of space, but at a different speed of sound. This can only be explained if the loop has substructuring (either consisting of shells at different temperatures or parallel threads of different temperature) at a scale of roughly below 3600 km. The SXT sequence was not useful because the loops are not emitting in this temperature range. This study clearly shows the importance of simultaneous observations in two different temperature bandpasses that are close enough to observe the same coronal structure.

Although the whole fan of loops support slow waves, we focus on one particular loop, in which a clear example of a PD is visible in the TRACE dataset. Figure 4 shows the field of view of the TRACE sequence and the selected loop. Over the observed fraction of the loop length, the loop cross-section increases by a factor of four. We assume that this is also true for each loop substructure. The intensity is measured as a function of time along the loop path where we integrate transversly within the path, over 2500 km, to improve the signal-to-noise ratio and to better capture the loop dynamics. It is not trivial to correctly track the loop along its length because the loops are closely spaced and overlapping, especially near the footpoints. We use the fact that the propagating PD outlines the loop position as a guide. It is not possible to determine the contribution of the loop to the total measured intensity and thus we contribute the full intensity to the loop.

The intensity variations along the loop path are extracted by subtracting a loop intensity background. Figure 5 shows an example of the intensity variations along the loop path as a function of time, where in each point a linear intensity profile has been subtracted. It shows that the loop is dynamic, especially near the loop footpoint (situated at 7 Mm along the path). In this diagram, the PDs appear as inclined, straight, parallel lines, with a quasi-periodicity of 5 to 20 minutes. The slope represents the projected propagation speed. To study in detail the intensity contribution of a single PD, the loop background intensity is subtracted more carefully. We select the bright PD that starts around 17h13, and measure the intensity variation following the propagation of the PD (comparing with our analytical model, his corresponds to keeping $\xi = z - C_s t$ constant) and integrating the signal, in time, between the two thick white lines. The projected propagation speed of the PD is 90 ± 10 km s^{-1}. This corresponds to an angle of 54 ± 5 degrees between the loop and the solar surface. Figure 7 shows the loop intensity and the relative loop intensity as a function of projected distance. Because we attributed the whole intensity to the loop, the relative loop intensity is probably underestimated. The relative intensity decreases with distance (height) with an e-folding length of roughly 45 Mm. Around a distance of 30-35 Mm along the loop path the relative intensity is enhanced by 1 to 2 percent. This is due to a transient brightening below the loop. The dashed lines are the noise level, which consist of the photon and CCD readout noise. From a distance of 70 Mm onwards the signalconsists only of noise and cosmic ray hits.

4. DISCUSSION

The relative intensity profile in Figure 7 represents the wave amplitude evolution with projected distance. This profile is copared with Expression (7). For this we consider that the intensity is proportional to ρ^2. For small amplitudes, the relative intensity amplitude is equal to $2\hat{V}/C_s$. The dot-dashed line in Figure 7 represents a best fit of the analytical model to the observation, where the footpoint amplitude, dissipation coefficient ηk^2 and the loopcross-section are varied. The observationally determined projection angle is used. We find $\eta k^2 = 3.0 \pm 1.5\ 10^{-8}$ m^{-1}. If we take k corresponding to a slow wave of a period of 5 and 20 minutes, we obtain a value for the dissipation coefficient of $\eta = 1.5 \pm 0.8$Mm and $\eta = 24 \pm 12$ Mm, respectively. This corresponds remarkably well to the theoretical expectations. It also indicates that the wave dynamics do not occure isothermally. This study proofs the feasability to determine prop-

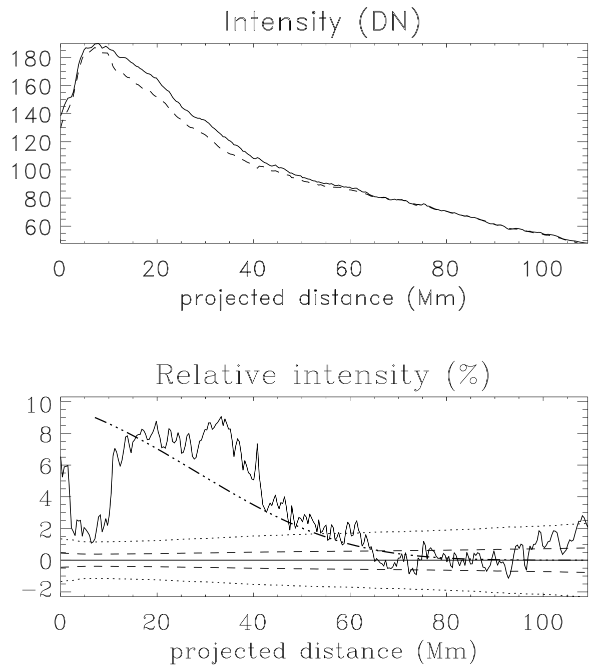

Figure 7. top: intensity profile as a function of projected distance along the selected loop path, following the propagation the PD. The dashed line is the loop background intensity profile. bottom: the relative intensity perturbation. dashed line: noise level, dotted line: three times the noise level, dot-dashed line: a best theoretical fit using Expression (7).

erties of the solar corona using slow magneto-acoustic waves as a probe. The capability of simultaneaous observations at different temperature bandpasses is of great use. For one the temperature dependency of the dissipation coefficient can be measured. With the current JOP80 sequences, only one wave PD was found with a large enough amplitude for studying its amplitude evolution. It seems clear that, eventhough a more clearly isolated loop will improve matters, the issue of a good signal-to-noise ratio as well as a fast cadence is of importance. For the detection of the intensity perturbation the exposure time Δt needs to be in the interval

$$\frac{\mathrm{SNR}^2\, d^2}{A_{sun}\, A_{eff}\, P_0\, a} < \Delta t < \frac{\ell}{V_{prop}} , \qquad (9)$$

where SNR, d, A_{sun}, A_{eff}, P_0 and a are the signal-to-noise level, distance to the Sun, pixel area, effective area of the instrument, luminosity of a solar feature and the relative amplitude of the wave respectively. ℓ is the typical length-scale of the wave, which needs to be larger than the resolution 2 $A_{sun}^{1/2}$. V_{prop} is the wave's propagation speed. The exposure time needs to be long enough in order for a significant signal to be build and the time cadence (and hence the exposure time) needs to be short enough to track the wave dynamics as well as minimizing motion blurring (which actually decreases the observed wave amplitude, so that longer exposures are needed). In comparison to TRACE and EIT, the High Resolution Imager (HRI) on board of the Solar Orbiter observes at a distance which is five times closer to the sun. This means a 25 times shorter exposure time to observe a feature at the same signal-to-noise level, spatial resolution and instrument quality. TRACE and EIT have typical exposure times of 10-20 s. To observe the same slow magneto-acoustic waves only an exposure times around or below one second is required. On the other hand, with an exposure time of 10 s a wave with an amplitude of ten time smaller can be observed. The spatial resolution of HRI will be 10 times better than that of TRACE, but this is not to our full advantage since a four times longer exposure time is needed to reach, at full resolution, the same level of signal-to-noise. Pixel rebinning therefore will be required. In its strictest form, if we take ℓ equal to the resolution, for a propagation speed of around 200 km s^{-1} (slow magneto-acoustic waves) and 2000 km s^{-1} (fast magneto-acoustic waves), we need a time cadence below 0.5 s and 0.05 s respectively. In order to optimally profit from the full resolution and to observe wave intensity perturbations in the order of 10 %, the instrument's effective area needs to improve by a factor of 100 for slow magneto-acoustic waves and 1000 for fast magneto-acoustic waves. If we permitt motion blurring (chosing ℓ to be tens of pixel lenghts), an improvement of a factor 10, respectively 100, is required. At the same time the detector's readout time needs to become shorter. The effective area may be increased by improving the detector'ssensitivity. This may be brought about by the use of novel type of detector's, such as proposed in the project Blind to Optical Light Detectors (see the contribution of Hochedez *et al.* to this workshop). On the other hand the available cadence and sequence duration is also constrained by telemetry, which is an important issue regarding the distance between Solar Orbiter and Earth.

ACKNOWLEDGEMENTS

The authors would like to thank the whole JOP 80 team for their contribution to this unique data set. E. Verwichte and J.-F. Hochedez would like to acknowledge the support of the Belgian Federal Services of Scientific, Technical and Cultural Affairs (SSTC/DWTC).

REFERENCES

Aschwanden, M.J., Fletcher, L., Schrijver, C.J. and Alexander, D. (1999): Coronal loop oscillations observed with the Transition Region and Coronal Explorer. *Ap.J.*, Vol. 526, pp. 1026-1045.

Berghmans, D. and Clette, F. (1999): Active region EUV transient brightenings - First results by EIT of SoHO JOP80. *Solar Phys.*, Vol. 186, pp. 207-229.

Berghmans, D., McKenzie, D. and Clette, F. (2001): Active region transient brightenings: A simultaneous view by SXT, EIT and TRACE. *Astron. Astrophys.*, Vol. 369, pp. 291-304.

Braginskii, S.I.(1965): Transport processes in a plasma. *Rev. Plasma Phys.*, Vol. 1, pp. 205-309.

Bray, R.J., Cram, L.E., Durrant, C.J. and Loughhead, R.E. (1991): Plasma loops in the solar corona, *Cambridge University Press, Cambridge*.

DeForest, C.E. and Gurman, J.B. (1998): Observation of quasi-periodic compressive waves in solar polar plumes. *Ap.J.*, Vol. 501, pp. L217-L220.

De Moortel, I., Ireland, J. and Walsh, R.W. (2000): Observation of oscillations in coronal loops. *Astron. Astrophys.*, Vol. 355, pp. L23-L26.

Nakariakov, V.M., Verwichte, E., Berghmans, D. and Robbrecht, E. (2000): Slow magnetoacoustic waves in loops. *Astron. Astrophys.*, Vol. 362, pp. 1151-1157.

Ofman, L., Romoli, M., Poletto, G., Noci, G. and Kohl, J. L. (1997): Ultraviolet Coronagraph Spectrometer observations of density fluctuations in the solar wind. *Ap.J.*, Vol. 491, pp. L111-L114.

Ofman, L., Nakariakov, V.M. and Sehgal, N. (2000): Dissipation of slow magnetoacoustic waves in coronal plumes. *Ap.J.*, Vol. 533, pp. 1071-1083.

Robbrecht, E., Berghmans, D. and Poedts, S. (1999): Active region transient brightenings. *Proceeding of the 8th SoHO Workshop, Paris, June 1999*, ESA SP-446, pp. 575-578.

Robbrecht, E., Verwichte, E., Berghmans, D., Hochedez, J.-F., Poedts, S. and Nakariakov, V.M. (2001): Slow magnetoacoustic waves in coronal loops: EIT and TRACE. *Astron. Astrophys.*, Vol. 370, pp. 591-601.